Surface Modification of Ti45Nb Alloy with an Alkylphosphonic Acid Self-Assembled Monolayer

G. Zorn,[†] I. Gotman,[†] E. Y. Gutmanas,*[,†] R. Adadi,[‡] G. Salitra,[‡] and C. N. Sukenik[‡]

Faculty of Materials Engineering, Technion, Haifa 32000, Israel, and Department of Chemistry, Bar-Ilan University, Ramat-Gan, Israel 52900

Received March 3, 2005. Revised Manuscript Received May 22, 2005

A new low-modulus β Ti−Nb alloy with low elastic modulus and excellent corrosion resistance is currently under consideration as a surgical implant material. The usefulness of such materials can be dramatically enhanced if their surface structure and surface chemistry can be controlled. This control is achieved in two stages. Electropolishing and anodic oxidation of the Ti45Nb alloy provide a surface with a uniform oxide layer that is a mixture of TiO_2 and Nb_2O_5. The impact of each of these two steps on the morphology of the surface and on the thickness and chemistry of the oxide layer has been assessed. In addition, as a first step toward controlling the surface chemistry of this material, a self-assembled monolayer (SAM) based on hexadecylphosphonic acid (HDPA) is attached to the anodized surface. The SAM is characterized based on its wetting properties and by Fourier transform infrared (FTIR) and X-ray photoelectron spectroscopy (XPS) analysis. Using variable angle XPS analysis, detailed information is obtained about the orientation and structure of the SAM, its thickness, and the chemistry of its interaction with the metal oxide surface of the alloy. Further support for the creation of a true monolayer film is obtained from FTIR measurements on a model oxide surface analogous to that of the alloy. This is the first report of SAM attachment to this alloy and opens the possibility of monolayer control of its biocompatibility.

Introduction

The use of titanium and its alloys as biomaterials is increasing due to their relatively low modulus and good corrosion resistance. Also, titanium is remarkably compatible with human tissue as compared to other metals. These properties were the driving force for the early introduction of commercially pure (cp) Ti and $\alpha+\beta$ (Ti−6Al−4V) alloys as well as for the more recent development of new metastable β titanium alloys. Ti−Nb alloys are especially noteworthy due to their remarkably low elastic modulus and excellent corrosion resistance.[1,2]

Since the biological response to an implanted biomaterial is influenced by the surface properties of the materials at a molecular level,[3−5] the interaction between an implant and its surrounding tissue can often be controlled by modifying the chemical and/or physical properties of the implant surface. Self-assembled monolayers (SAMs) are useful for modifying surface chemistry and/or attaching molecules to surfaces. The SAMs provide chemically and structurally well-defined surfaces that can often be manipulated using standard synthetic methodologies.[6] SAM attachment to a metal or alloy surface depends in large part on the composition and reactivity of the surface. It is therefore important to control the surface onto which a SAM will be attached with respect to its chemical composition and microstructure, as they will determine the quality of the SAM in terms of its stability, degree of coverage, and order.

Thiol on gold SAMs has been particularly well-studied,[7,8] as have siloxane-anchored SAMs.[9] More recently, alkyl phosphates have been used to provide an ordered monolayer on tantalum oxide surfaces[10,11] and alkylphosphonic acids have been used to coat the native oxide surfaces of metals (and their alloys) including tin,[12] iron,[13] steel,[14] aluminum,[13−15] copper,[14] and titanium.[16]

Several procedures have been reported for obtaining alkylphosphonic acid films on different metals. ZrO_2 was found to be a more suitable substrate than TiO_2 or Al_2O_3 for the formation of ordered SAMs. This deposition was

* To whom correspondence should be addressed. E-mail: gutmanas@tx.technion.ac.il.
[†] Technion.
[‡] Bar-Ilan University.

(1) Rosenberg, R.; Starosvetsky, D.; Gotman, I. *J. Mater. Sci. Lett.* **2003**, *22*, 29.
(2) Godly, R.; Starosvetsky, D.; Gotman, I. *J. Mater. Sci.: Mater. Med.* **2004**, *15*, 1073.
(3) Kasemo, B. *J. Prosthet. Dent.* **1983**, *49*, 832.
(4) Ratner, B. D. *Ann. Biomed. Eng.* **1983**, *11*, 313.
(5) Gristina, A. G. *Science* **1987**, *237*, 1588.
(6) Balachander, N.; Sukenik, C. N. *Langmuir* **1990**, *6*, 1621.
(7) Bain, C. D.; Troughton, E. B.; Tao, Y. T.; Evall, J.; Whitesides, G. M.; Nuzzo, R. G. *J. Am. Chem. Soc.* **1989**, *111*, 321.
(8) Dubois, L. H.; Nuzzo, R. G. *Annu. Rev. Phys. Chem.* **1992**, *43*, 437.
(9) Ulman, A. *Chem. Rev.* **1996**, *96*, 1533.
(10) Brovelli, D.; Hähner, G.; Ruiz, L.; Hofer, R.; Kraus, G.; Waldner, A.; Schlösser, J.; Oroszlan, P.; Ehart, M.; Spencer, N. D. *Langmuir* **1999**, *15*, 4324.
(11) Textor, M.; Ruiz, L.; Hofer, R.; Rossi, A.; Feldman, K.; Hähner, G.; Spencer, N. D. *Langmuir* **2000**, *16*, 3257.
(12) Fang, J. L.; Wu, N. J.; Wang, Z. W.; Li, Y. *Corrosion* **1991**, *47*, 169.
(13) Gawalt, E. S.; Lu, G.; Bernasek, S. L.; Schwartz, J. *Langmuir* **1999**, *15*, 8929.
(14) Van Alsten, J. G. *Langmuir* **1999**, *15*, 7605.
(15) Nitowski, G. A.; Wiserman, L. F.; Wefers, K. *Chem. Abstr.* **1994**, *121*, 20979w.
(16) Gawalt, E. S.; Avaltroni, M. J.; Koch, N.; Schwartz, J. *Langmuir* **2001**, *17*, 5736.

10.1021/cm050477f CCC: $30.25
Published on Web 07/07/2005

effectively done from a methanol−water mixed solvent.[17] The adsorption of octadecylphosphonic acid on TiO_2 and on Al_2O_3 was also successful, though it yielded films with significant disorder.[17] Using a different procedure (below), Schwartz et al.[16] reported assembling a strongly surface-bound film of octadecylphosphonic acid onto a TiO_2 surface.

In the work reported herein, a SAM of hexadecylphosphonic acid (HDPA) was attached to the oxide surface of β Ti45Nb (solid solution of 45 wt % of Nb in Ti). A primary objective of the work was to optimize surface preparation procedures so as not to degrade the surface of the alloy while reproducibly providing a sufficiently reactive surface so as to support a stable, well-ordered phosphonate-anchored SAM. The deposition procedure developed by Schwartz[16] provided a useful starting point for our efforts, though differences in the procedure used and/or differences in reactivity between the β Ti45Nb alloy surface and that of pure TiO_2 may alter the degree to which a true monolayer film is obtained. The SAMs obtained were extensively characterized, and a detailed picture of the SAM−oxide interface has emerged. Moreover, in an effort to better define the monolayer nature of our alkylphosphonate surface film, a model system based on the deposition of a thin, uniform mixed Ti/Nb oxide on a double side polished silicon wafer has been developed. It allows us to characterize the phosphonate film in ways impossible on the surface of the bulk alloy.

Materials and Methods

1. Substrates. Ti45Nb was purchased from Performance Materials and Alloys (NJ, U.S.A.). The 1×1 cm^2 and 1×2.5 cm^2 Ti45Nb (3 mm thick) samples were first ground with 60, 120, 240, 600, and 1200 grit silicon carbide paper, followed by sonication in methanol. Electropolishing[18,19] was done in an electrolyte consisting of a mixture of 540 mL of methanol, 350 mL of *n*-butanol, and 60 of mL perchloric acid, held at −30 °C. The current density was ~200 A/cm^2, and the electropolishing times were 5−7 min. The sample was then sonicated with CH_2Cl_2, acetone, and ethanol for 15 min each and dried in a stream of dry air. Anodic oxidation[18,19] was done in 1 M H_2SO_4 electrolyte at room temperature. The current density was kept at 60 mA/cm^2 during the initial part of the anodization during which the potential was allowed to increase from 5 V to a preset value of 100 V. When the preset voltage was reached (after about 1 min) the anodization was stopped. The anodized samples were sonicated with CH_2Cl_2, acetone, ethanol, and deionized water for 15 min each and then dried in a stream of dry air.

The substrate needed for our model oxide interface is based on a double side polished silicon wafer ($60 \times 10 \times 0.45$ mm; n-doped; {100}) that was made into a suitable internal reflection element (IRE) for Fourier transform infrared attenuated total reflectance (FTIR-ATR) spectroscopy by polishing its two short edges to a 45° angle to create a parallelogram prism. It was cleaned ultrasonically in chloroform, acetone, and ethanol (10 min each) and, finally, using a UV ozone cleaner (UVOCS) for 15 min. A thin film of Ti45Nb was sputtered onto each side of the wafer using a magnetron sputtering source energized by a direct current power supply operating in power control mode in a HV-based system. The target was a disk (50 mm diameter, 3 mm thick) of Ti−45%Nb. The base pressure was below 5×10^{-6} Torr before introduction of the argon sputtering gas at 5×10^{-3} Torr. The metal-coated wafer was oxidized by heating in air at temperatures up to 400 °C, for times up to 30 min.

2. SAM Deposition. A solution of HDPA[20] (17 mg) in tetrahydrofuran (THF; 40 mL) was prepared and heated (with stirring) at 70 °C under nitrogen. Into this solution were immersed the electropolished and the electropolished/anodized Ti45Nb coupons. They were kept in the solution for 2 h, and the temperature was then raised to 120 °C, causing the THF to boil out (~2 h). The samples are left open to air at 120 °C for an additional 16 h. They were rinsed in fresh, dry THF and then dried with filtered N_2 and characterized. A second coating often resulted in improved coverage (see text).

3. Optical Microscopy. Optical Microscope images were taken using an Axiophot photomicroscope (Zeiss, Germany) and SIS image processing software (Soft Imaging System, Germany).

4. Auger Electron Spectroscopy (AES). AES analyses were performed with a scanning Auger microprobe (Thermo V G Scientific Microlab 350). A primary electron beam energy of 10 keV and beam current of 10 nA were used. The 4 keV Ar^+ ions were used for depth profile measurements. The depth scale was calibrated using a 100 nm Ta_2O_5 standard. The oxide thickness was measured by ascertaining when the oxygen peak reached half its maximum concentration (range of error is about 30%).

5. Atomic Force Microscope (AFM). AFM measurements were preformed with an Autoprobe CP AFM (Park Scientific Instruments, U.S.A.) operated in the contact mode. AFM scans were done with CS11/50 ultrasharp Si tips, coated with W_2C. Their nominal radius of curvature was 50 nm. The scan rate was 1 line/s. The AFM images contained 256×256 pixels. They were taken in the region of the grain boundary grooves, with the scanning direction perpendicular to the groove.

6. X-ray Photoelectron Spectroscopy (XPS). XPS analyses were performed on a Sigma probe X-ray photoelectron spectrometer from Thermo V. G. Scientific using a monochromatized aluminum anode X-ray source (Al Kα 1486.68 eV). Spectra were taken at three emission angles: 37 ± 30° (standard mode), 15.5 ± 7.5° (surface-sensitive mode), and 59.5 ± 7.5° (bulk mode) takeoff angles with respect to the surface. The latter two modes were particularly useful in characterizing the HDPA SAM coated Ti45Nb. Samples were analyzed with a pass energy of 100.0 eV for survey scans and 20.0 eV for high-resolution elemental scans. The energy scale was calibrated by referencing the main hydrocarbon peak which was set at a binding energy of 285.0 eV.[21]

7. FTIR Spectroscopy. FTIR spectra were measured using a Bruker Vector 22 equipped with a mercury cadmium telluride detector. In one method, electropolished (and anodized) samples were placed in a Bruker grazing angle accessory. The angle of incidence was 55°. Prior to collection of the spectra, the sample compartment was purged with dried air for 10 min. The spectra (1000 scans) were then acquired using 4 cm^{-1} resolution and triangular apodization. Each spectrum of the HDPA SAM coated samples was obtained by subtracting a background obtained using a clean, bare alloy sample.

In a second method, FTIR-ATR spectroscopy was applied to the model substrate with a TiNb oxide film on a double-side

(17) Gao, W.; Dickinson, L.; Grozinger, C.; Morin, F. G.; Reven, L. *Langmuir* **1996**, *12*, 6429.
(18) Lausmaa, J.; Kasemo, B.; Mattsson, H.; Odelius, H. *Appl. Surf. Sci.* **1990**, *45*, 189.
(19) Lausmaa, J.; Kasemo, B.; Rolander, U.; Bjursten, L. M.; Ericson, L. E.; Rosander, L.; Thomsen, P. In *Surface Characterization of Biomaterials*; Ratner, B. D., Ed.; Elsevier: Amsterdam, 1988; p 161.
(20) Sahoo, Y.; Pizem, H.; Fried, T.; Golodnitsky, D.; Burstein, L.; Sukenik, C. N.; Markovich, G. *Langmuir* **2001**, *17*, 7907.
(21) Tosatti, S.; Michel, R.; Textor, M.; Spencer, N. D. *Langmuir* **2002**, *18*, 3537.

polished silicon wafer. HDPA was deposited onto this oxide surface using the procedure described above for SAM formation on the surface of the alloy samples. FTIR-ATR spectra of the adsorbed HDPA films were recorded on a Bruker Vector 22 FTIR, with data acquisition and analysis using Opus 3.1 software. Typically, 1000 scans at 4 cm^{-1} nominal spectral resolutions were collected, and the spectrum was obtained by subtracting a background of the initial oxide-coated ATR prism.

8. Contact-Angle Measurements. Contact angle values (average of at least five measurements taken at different points on the surface) were measured using a Rame-Hart model 100 contact angle goniometer.

9. Ellipsometry. Thickness measurements of the metal, metal oxide, and organic films were made on a Woollam M-44 variable angle spectroscopic ellipsometer with a quartz tungsten halogen 50 W source and an 8 mm spot. Data were processed using WVASE32 software v3.154 (hardware version 11.900) after calibration of the system using a standard Si wafer with a 25.0-nm SiO_2 layer as a reference. The data were collected at angles of incidence from 66 to 70° (2° increments) and at 44 fixed wavelengths between 650 and 1108 nm and by fitting (as needed) the refractive index over the entire range of wavelengths.

The thicknesses of the initially sputtered metal layer and of the TiO_2/Nb_2O_5 layer were calculated using a best-fit refractive index. The thickness of the HDPA layer was calculated using an assumed refractive index of 1.45. The theoretical thickness of the HDPA layer was estimated from the length of the fully extended chain of a HDPA molecule, calculated using PCMODEL v7 (Serena Software).

Results and Discussion

Reproducible creation of a high-quality SAM requires an initial substrate surface with as little contamination as possible. Moreover, SAM characterization (thickness, wetting, FTIR) is best done on surfaces that are as smooth as possible. Thus, a smooth, clean surface had to be prepared on the polycrystalline Ti45Nb samples. Also, because the composition and structure of the surface influences SAM bonding, a well-defined and reproducible surface preparation, together with a good understanding of the Ti45Nb surface properties, was needed. Mechanical polishing with a series of SiC papers, diamond polish, and alumina powder (average particle size 0.05 μm) provided a surface that was contaminated with traces of Al. However, electropolishing and anodic oxidation after SiC polishing provided a reflective, smooth surface, free of contamination. The electrochemical procedures used in the literature for cp Ti[18,19] were found to be appropriate for Ti45Nb.

1. Characterization of the Ti45Nb Surface. Optical microscope images of electropolished Ti45Nb and of Ti45Nb that had been both electropolished and anodized are shown in parts a and b of Figure 1, respectively. In both cases, grain boundaries can be seen clearly and anodic oxidation does not seem to influence the surface grain size.

AFM images (contact mode) of the electropolished samples were recorded, before and after anodization. The three-dimensional AFM image given in Figure 2 shows the surface morphology of electropolished Ti45Nb after anodization. The height profiles (before and after anodization) are given in Figure 3. It is clear that, while anodization does not significantly change the grain size, it increases surface roughness.

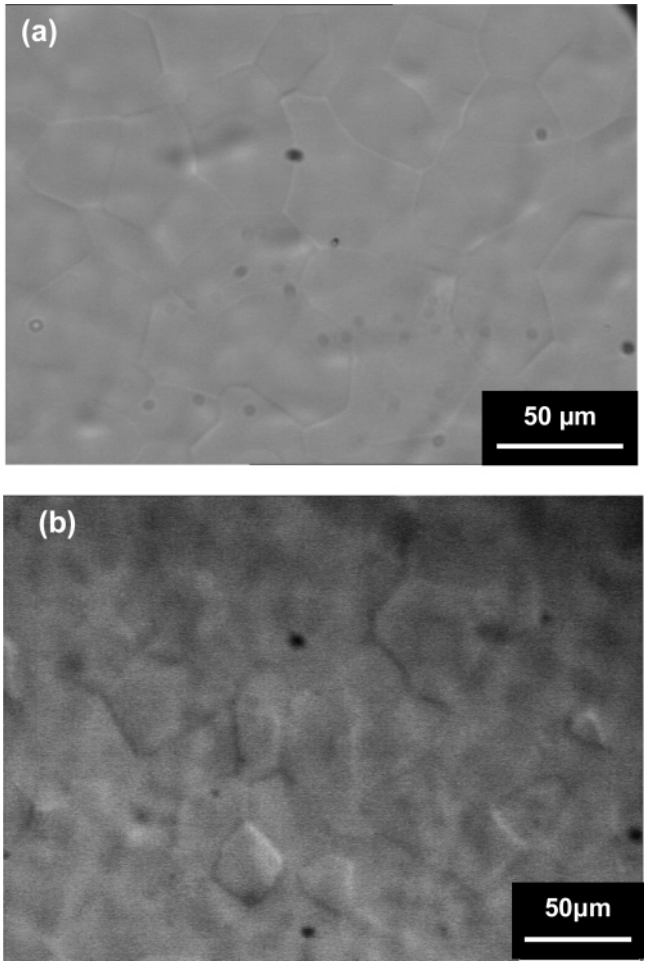

Figure 1. Optical microscope images of the electropolished Ti45Nb surface (a) before and (b) after anodic oxidation.

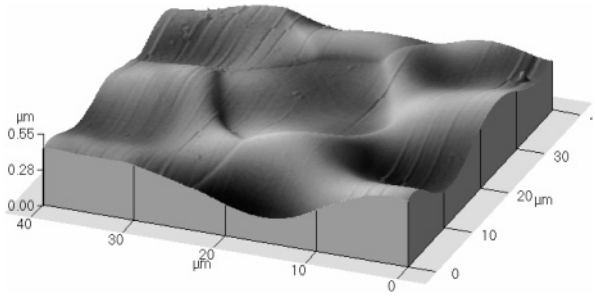

Figure 2. AFM three-dimensional image of the electropolished Ti45Nb surface after anodization (contact mode).

AES was used to depth profile the alloy and to estimate the oxide thickness on the electropolished Ti45Nb, before and after anodization. The depth profile of Nb MNN, Ti LMM, O KLL, and C KLL was measured. The oxide thickness before anodization is estimated to be 10 nm. After anodization, it is ~280 nm (Figure 4), with the surface carbon disappearing after only a few nanometers and with the ratio of Ti/Nb staying relatively constant throughout the thickness of the surface oxide.

The composition of the outermost surface of electropolished Ti45Nb before and after anodization was examined by XPS. The results are summarized in Table 1. These analyses suggest that the Ti/Nb ratio in the alloy surface is somewhat reduced by anodization (1.93 compared to 1.65).

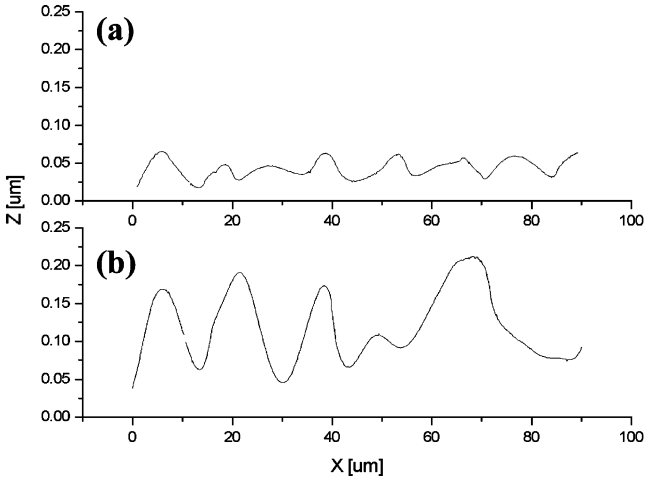

Figure 3. AFM height profiles of the electropolished Ti45Nb surface (a) before and (b) after anodic oxidation.

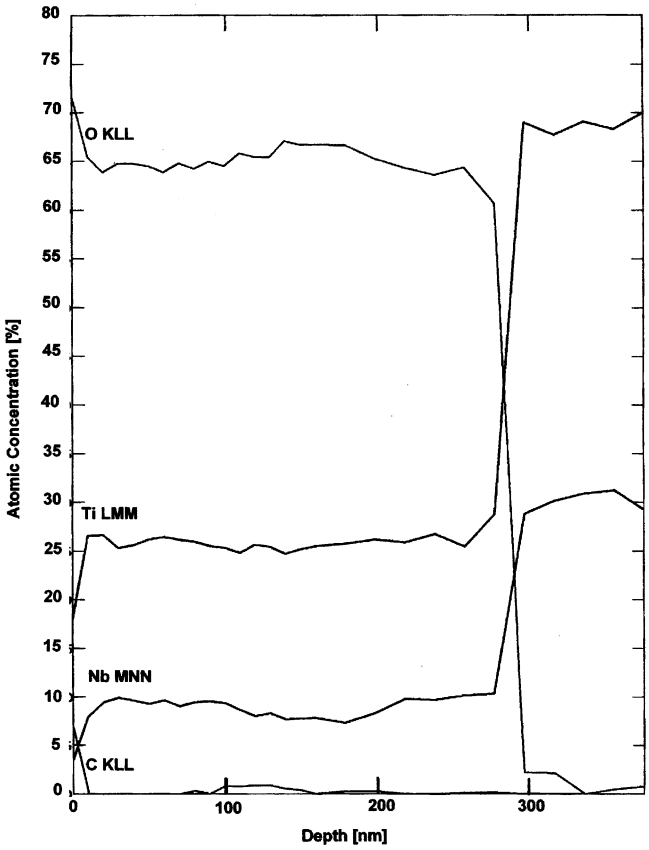

Figure 4. AES depth profile of electropolished Ti45Nb after anodization.

Table 1. XPS Composition (Standard Mode) of Electropolished Ti45Nb

peak	BE [eV]	assignment[22]	atom % before anodization	atom % after anodization
Ti($2p_{3/2}$)	458.6	TiO_2	11.8	11.4
Nb($3d_{5/2}$)	207.1	Nb_2O_5	6.1	6.9
O(1s)	530.1	TiO_2, Nb_2O_5	49.2	52.0
C(1s)	285.0−288.0	carbon contamination	32.8	29.8

2. Creation and Characterization of the HDPA SAM. Phosphonic and phosphoric acids are known to interact strongly with transition metal oxides such as tantalum oxide (Ta_2O_5),[23] niobium oxide (Nb_2O_5),[23] and titanium oxide (TiO_2).[16,21] Long-chain phosphonic acids attach to the metal oxides (which are basic hydroxyl surfaces) via acid−base interactions that anchor the molecule to the surface. Self-assembly of HDPA on the Ti45Nb alloy is done by adsorption and solvent evaporation. That is, the oxide surface is wetted with a solution of the phosphonic acid in an organic solvent (THF) and the solvent is evaporated. Subsequent heating gives a stable surface film that resists removal (ethanol sonication). We have found that repeating the deposition procedure twice on Ti45Nb improves surface coverage of HDPA and the order of the film. A similarly improved film by repeated treatment has been found for alkylphosphonates on titanium oxide[16] and on mica.[24] On the surface of Ti45Nb, once excess (unbound) phosphonic acid is removed, the remaining film is uniform and well-ordered (see below).

The wetting properties of the SAM coated Ti45Nb samples provided a simple assay of the quality of the HDPA SAM. Measurements of advancing and receding contact angles showed that very hydrophobic and relatively uniform SAMs could be formed on both anodized and unanodized samples. An advancing contact angle of $\geq 110°$ and a hysteresis of less than 5° are the standard diagnostics for a uniform, hydrophobic SAM on a smooth substrate. The roughness of our samples precludes achieving such small hysteresis values. The contact angle measurements (adv/rec) for HDPA SAM coated samples were $110°/100° \pm 3°$ and $110°/94° \pm 5°$ for anodized and unanodized samples, respectively. The smaller hysteresis and smaller error bars for the anodized samples are consistent with a somewhat higher degree of order, more complete surface coverage, and somewhat higher packing density (see FTIR analysis below). However, even without anodization, formation of a robust surface film is achieved. We also note that the properties of our films on the mixed Ti−Nb oxide surface are consistent with those of the films reported for alkyl phosphate monolayers on each of these oxides separately (advancing contact angles of 110−111°).[23]

The FTIR spectra of the coated alloy samples provide additional insight. The methylene stretching frequencies are an important diagnostic for the completeness and packing of the SAM. Their intensity reflects the coverage, and their position reflects SAM order. Asymmetric C−H stretches of 2917 cm^{-1} or less indicate an ordered, more crystalline film with its methylene groups predominantly in an all-trans conformation.[17] Absorptions at 2922 cm^{-1} or higher reflect a disordered (liquidlike) film. Similarly, lower-frequency symmetric C−H stretches ($\sim$2850 cm^{-1}) suggest a higher degree of order. The external reflection FTIR spectra of HDPA SAM coated Ti45Nb are shown in Figure 5. While the external reflection measurement is sensitive to surface roughness which might influence the signal-to-noise ratio and/or the absolute intensity of the peaks, it is clear that the HDPA SAM on the anodized substrate is a better-ordered film. The observed peaks at 2916 and 2848 cm^{-1} suggest a well-ordered SAM. Higher frequencies and broader peaks for the C−H stretches of the SAM on the unanodized surface

(22) http://srdata.nist.gov/xps/ (accessed May 2005).
(23) Hofer, R.; Textor, M.; Spencer, N. D. *Langmuir* **2001**, *17*, 4014.
(24) Woodward, J. T.; Schwartz, D. K. *J. Am. Chem. Soc.* **1996**, *118*, 7861.

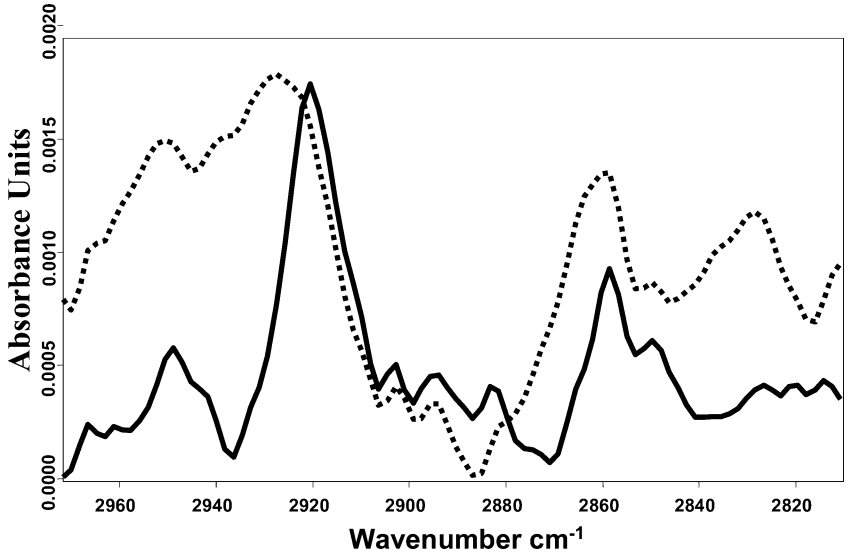

Figure 5. FTIR spectra of the HDPA SAM on (dotted line) electropolished and (solid line) anodized Ti45Nb.

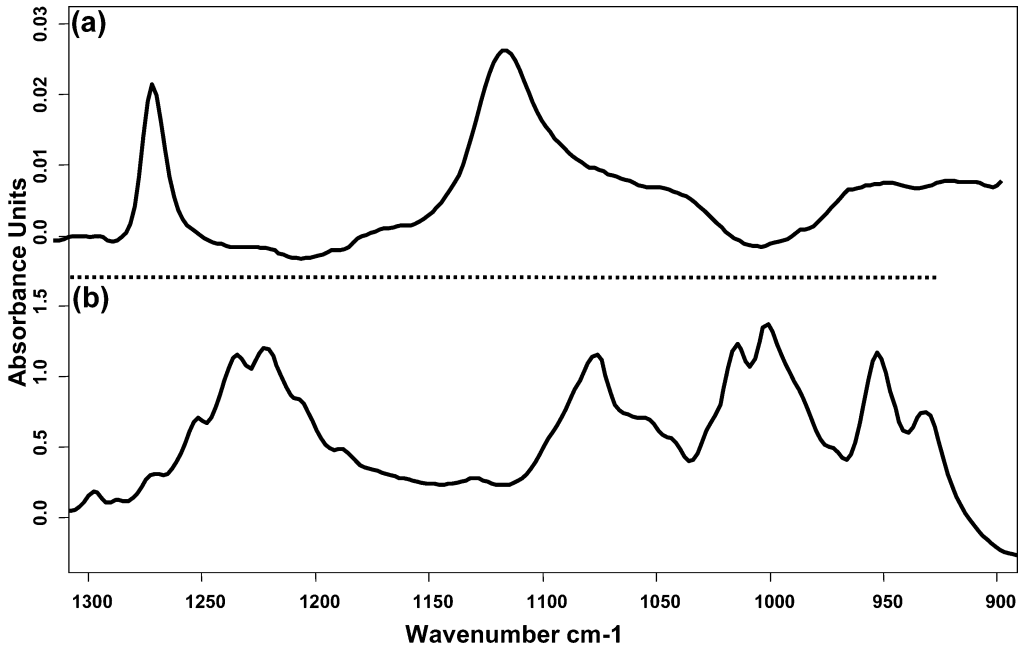

Figure 6. (a) External reflection FTIR spectra of HDPA SAM anodized Ti45Nb. (b) Transmission FTIR spectra of HDPA in a KBr pellet.

accentuate the difference in the order and packing of the SAMs.

Figure 6a shows the 900−1300 cm^{-1} spectral region of the external reflection FTIR spectra of HDPA SAM coated Ti45Nb alongside (Figure 6b) the same spectral region from a spectrum of the free phosphonic acid in a KBr pellet. It is clear that the peaks at 1264 and 1111 cm^{-1} are the result of phosphonate binding to the oxide surface and that the peaks of the free acid (as per Figure 6b around 1225, 1075, 1010, and 950 cm^{-1}) are essentially absent. These spectra clearly support the assertion that essentially all the phosphonic acid headgroups are bound to the oxide surface. Similar conclusions have been drawn for phosphonic acids attached to titanium substrates[13] and to ZrO_2 particles.[17]

XPS survey spectra of bare and HDPA SAM coated Ti45Nb probed the extent of SAM coverage. Figures 7 and 8 respectively show spectra collected at 59.5 ± 7.5° (bulk mode) and 15.5 ± 7.5° (surface-sensitive mode) takeoff angles. The sampling depth (Z), as determined by the relationship $Z \cong 3\lambda \sin\theta$, where λ is the attenuation length of the emitted photoelectrons, is ~82 Å for Ti($2p_{3/2}$) for the bulk mode. The λ value was determined experimentally over a kinetic energy range of 500−1500 eV to be λ [Å] = 9.0 + 0.022E_k [eV].[25]

As expected, the SAM coated samples show more prominent carbon peaks and evidence of phosphorus. In Figure 7, the Ti($2p_{3/2}$) and the Nb($3d_{5/2}$) peaks are smaller on the SAM coated sample, and in Figure 8 (surface-sensitive mode), they cannot be seen at all. The SAM allows XPS sampling down to the alloy substrate only at a high takeoff angle. This is good evidence that the HDPA SAM completely covers the Ti45Nb surface.

High-resolution XPS spectra provided a more precise analysis of surface composition. Gaussian−Lorenzian curve

(25) Laibinis, P. E.; Bain, C. D.; Whitesides, G. M. *J. Phys. Chem.* **1991**, *95*, 7017.

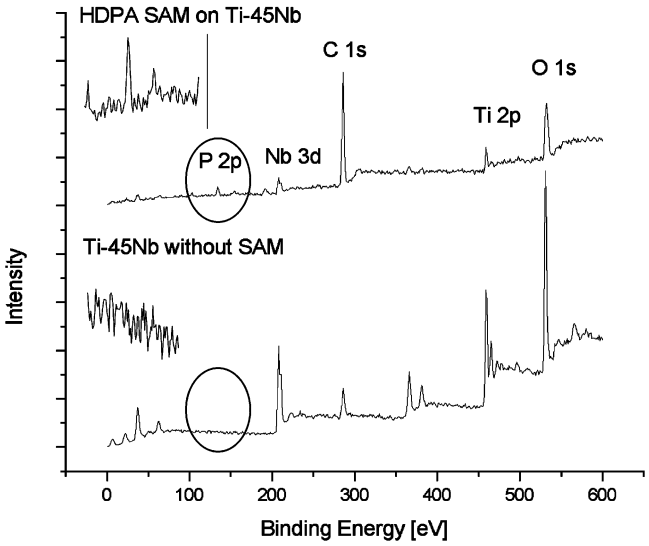

Figure 7. XPS survey spectra, bulk mode.

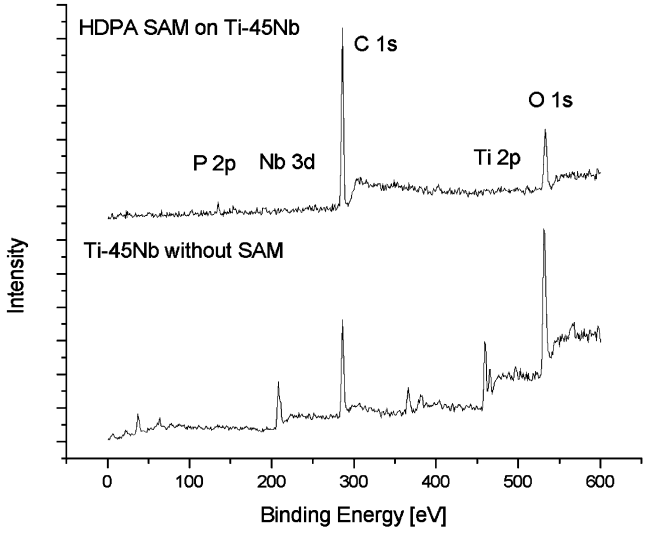

Figure 8. XPS survey spectra, surface-sensitive mode.

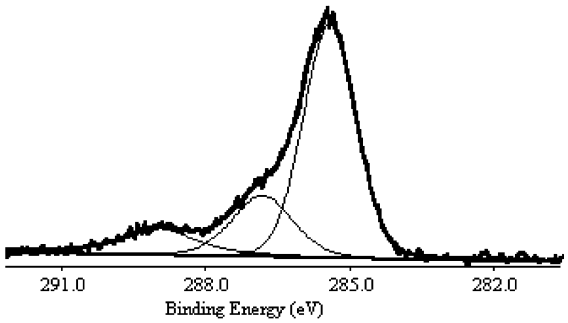

Figure 9. C(1s) high-resolution XPS of the bare anodized Ti45Nb.

deconvolution after linear background subtraction allowed investigation of the chemical state of the surface components. In Figure 9, the high-resolution C(1s) XPS spectrum (Table 1) of the bare anodized Ti45Nb (collected at the standard angle, i.e., 37°) is shown. Figure 10 shows high-resolution XPS spectra of the SAM coated samples. The C(1s) peak in surface-sensitive mode and the O(1s) peaks obtained in both surface-sensitive bulk modes are shown. They are assigned in Table 2.

A number of important observations emerge from this analysis. The C(1s) peak of the coated sample could be cleanly fitted with only alkyl carbons (285.0 eV; Figure 10a). The C(1s) peak on the uncoated sample (Table 1 and Figure 9) could not be fit in this way. This suggests that the surface contaminants on the bare Ti45Nb were comprised of multiple kinds of carbon-containing material, were exchanged by adsorbed HDPA molecules, and, thus, were removed. Along these same lines, the observed ratio of C:P in the surface-sensitive analysis of 80.6/5 or 16.1 is exactly what is to be expected for a SAM based on HDPA.

The O(1s) signal detected in the bulk mode was quite different from the one detected in the surface-sensitive mode (Figure 10b,c). The surface-sensitive mode signal could be nicely fit using only two peaks, while three were needed to fit the bulk mode signal. The peak that is observed only in the bulk mode (530.1 eV) corresponds to the surface metal oxides (TiO_2 and Nb_2O_5). The absence of this peak in the surface-sensitive mode and the fact that we only see the SAM in the surface-sensitive mode analysis are consistent with the SAM fully covering the surface. Confirmation that the HDPA coating is quite complete is based on the absence of the titanium and niobium peaks at the lower takeoff angle along with the ability to detect them at the higher takeoff angle.

The two O(1s) peaks detected in both bulk and surface-sensitive modes are associated with the phosphonic acid group (PO_3H_2). The peak at 531.9 eV can be assigned to P═O and P—O—Ti or P—O—Nb, while the peak at 533.0 eV is assigned to P—O—H.[11] These two peaks in the surface-sensitive mode measurement account for 14.4 atom % and are found in a ratio of 2.9/1 relative to the phosphorus signal. This is the molecular ratio expected (3/1) for a phosphonic acid group.

The ratios between the two oxygen peaks (at 531.9 and 533.0 eV) for the HDPA SAM on Ti45Nb are 2.5 and 3.4 in the bulk and surface-sensitive modes, respectively (Table 2). This ratio speaks to the details of the interaction of the phosphonate with the surface. For an unbound phosphonic group, the ratio between P═O and P—OH should be 0.5. XPS analysis of HDPA powder (Figure 11) indeed shows a value of 0.52 for the ratio between the oxygen peaks at 531.9 and 533.0 eV. The larger proportion of the peak at 531.9 eV (assigned also to P—O—Ti and P—O—Nb) in the O(1s) signal from HDPA SAM on Ti45Nb must be due to the transformation of most of the P—OH bonds (533.0 eV) to P—O—Ti or P—O—Nb bonds, suggesting covalent attachment of the HDPA molecules to the titanium−niobium oxide surface.

If a single phosphonate oxygen were connected to the surface and the other two were as P═O and P—OH, a ratio of 2:1 would be expected for the oxygen signals (531.9/533). The fact that it is greater than 2 argues that some HDPA molecules have two P—O—metal interactions and no P—OH. Such chelated (two-pronged) anchoring is likely important to the observed SAM stability. The change in this ratio from 2.5 in the bulk mode to 3.4 in the surface-sensitive mode may also suggest a model where both the P—O—H and the P—O—metal are closer to the surface than the P═O. It is also reasonable to suggest that the persistence of at least some P—O—H units may contribute cross-link stabilization

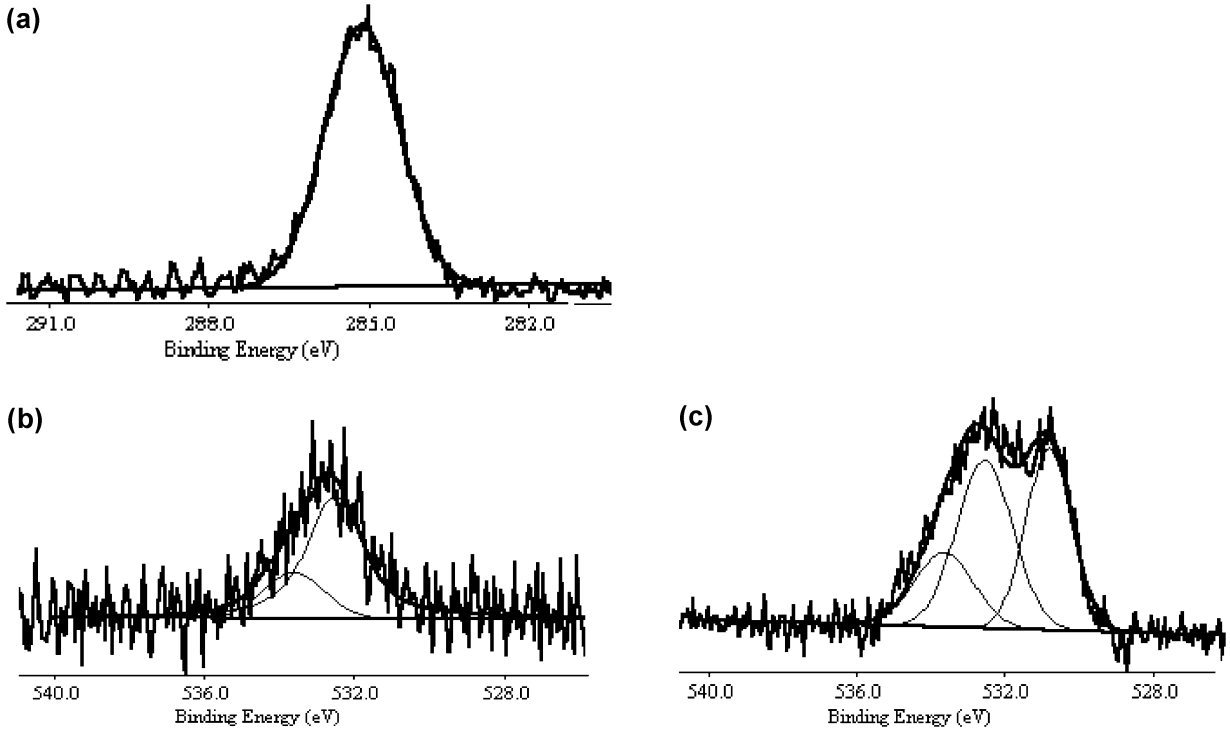

Figure 10. High-resolution XPS of the SAM coated sample in the (a) C(1s) surface-sensitive mode, (b) O(1s) surface-sensitive mode, and (c) O(1s) bulk mode.

Table 2. XPS Analysis of Surface Composition and Surface Chemical State

peak	binding energy [eV]	assignment[11,21,22,26]	bulk mode [atom %]	surface-sensitive mode [atom %]
C(1s)	285.0	CH_2; CH_3	71.3	80.6
O(1s)	530.1	TiO_2; Nb_2O_5	6.3	
	531.9	P═O; P—O—Ti; P—O—Nb	8.4	11.1
	533.0	P—O—H	3.4	3.3
$P(2p_{3/2})$	133.6	R—P(O)$(OH)_2$	6.7	5.0
$Ti(2p_{3/2})$	458.6	TiO_2	2.3	
$Nb(3d_{5/2})$	207.1	Nb_2O_5	1.6	

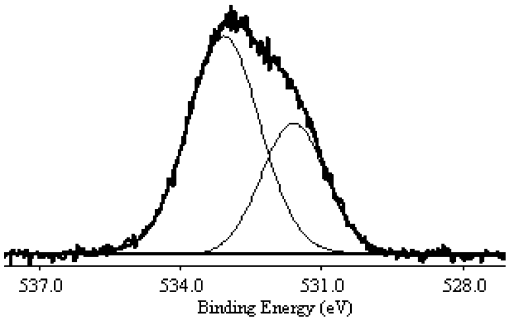

Figure 11. O(1s) high-resolution XPS of HDPA powder.

to the SAM by allowing for hydrogen-bond interactions between anchoring groups.

It is also possible to estimate the thickness of the SAM using XPS data from different takeoff angles.[27] The XPS intensity, I, from a smooth substrate covered by a thin film of thickness d is given by the equation $I = I_0 \exp[-d/(\lambda \sin \theta)]$ where I_0 is the photoelectron intensity from the clean substrate, θ is the emission angle (with respect to the surface), and λ is the attenuation length of the emitted photoelectrons from the substrate. The phosphorus, $P(2p_{3/2})$, is at the interface between the monolayer and the substrate so its signal at the two emission angles was used to estimate the thickness of the organic film. The intensities of the $P(2p_{3/2})$ used to determine the atomic percentage in Table 2 are 1705 and 500 cps for the bulk and surface-sensitive modes, respectively. The attenuation length, λ, calculated as described above, gives a value of 38.8 Å. The dependence between the intensity and the takeoff angle for $P(2p_{3/2})$ gives a thickness value, d, of 1.8 nm for the carbon chains above the phosphorus. This compares very favorably with the expected distance between the first and last carbon of a 16-carbon chain of 1.9 nm and speaks strongly for the monolayer character of the HDPA SAM.

These observations compare well with the model proposed[11] for alkyl phosphates on metal oxide surfaces and support a picture of an alkylphosphonate-anchored SAM on Ti45Nb with the phosphonates at the SAM—oxide interface in a well-defined orientation, with the alkyl chains in a "tails-up" configuration. Together with the hydrophobicity of the surface film, the ordering suggested by the FTIR, and the thickness calculated from XPS analysis at two emission angles, a consistent picture of a monolayer film on the oxide interface of the bulk alloy emerges.

Finally, an even more convincing proof of the monolayer nature of the adsorbed HDPA film was sought. The roughness of the real-world alloy precluded direct film thickness measurements (by ellipsometry) or nanometer resolution AFM measurements of film topography and roughness. So too, the bulk alloy prevented the application of ATR-FTIR in a way that would clearly identify a true monolayer. Thus, we created a model surface of TiO_2/Nb_2O_5 on a double-side

(26) Viornery, C.; Chvolot, Y.; Léonard, D.; Aronsson, B. O.; Péchy, P.; Mathieu, H. J.; Descouts, P.; Grätzel, M. *Langmuir* **2002**, *18*, 2582.
(27) Yamamoto, H.; Butera, R. A.; Gu, Y.; Waldeck, D. H. *Langmuir* **1999**, *15*, 8640.

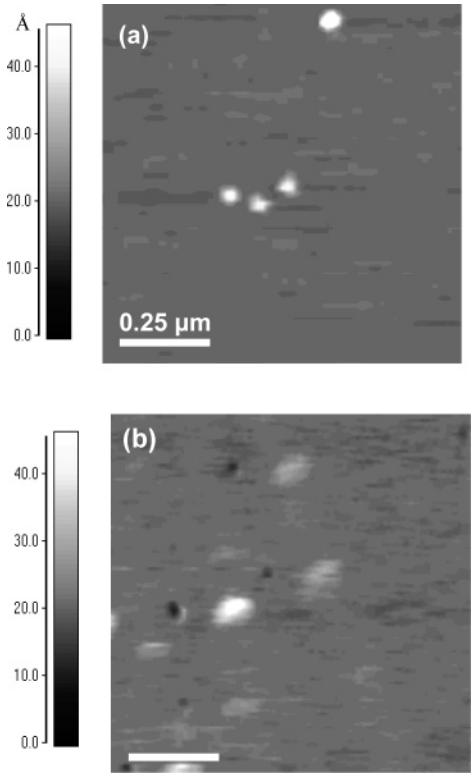

Figure 12. AFM micrographs (1 × 1 μm) of the TiNb layer on polished single-crystal silicon, before (a) and after (b) HDPA deposition.

polished silicon wafer that would allow such measurements, while preserving the chemical characteristics of the alloy surface.

Deposition (by sputtering) of a mixture of Ti and Nb metal onto both sides of a double-side polished silicon wafer (providing a sensitive IRE), followed by its oxidation, provided a TiO_2/Nb_2O_5 film (15−30 nm) on the polished silicon wafer surface. XPS analysis of the surface oxide showed a metal oxide composition of 54.6% Ti and 45.4% Nb, when the sputtered mixed-metal layer was made from an alloy target with a 55% Ti and 45% Nb composition.

It was important to keep the TiO_2/Nb_2O_5 layer as thin and as uniform as possible so as to minimize the perturbation of subsequent ellipsometry and FTIR measurements. While thickness measurements on the freshly deposited metal were difficult due to its spontaneous oxidation, deposition of ∼7−15 nm of metal gave uniform surface coverage that became a 15−30 nm oxide film upon air oxidation. The complete oxidation of both the titanium and the niobium was proven by XPS showing that no metal signals remained [Ti(2p) = metal 453.7 eV, oxide 458.6; Nb(3d) = metal 202.4 eV, oxide 207.1 eV].

The thicknesses (measured by ellipsometry) of the HDPA film on the TiO_2/Nb_2O_5 surface on the silicon wafer was 2.1 nm. The calculated length of the HDPA molecule in an extended chain conformation (hydrocarbon chain and phosphonic acid headgroup) is 2.2 nm. Considering the lack of information about the likely tilt of such films, we simply suggest that the measured thickness is reasonably consistent with a monolayer, rather than a multilayer, film.

AFM analysis (Figure 12) of the TiO_2/Nb_2O_5 surface on the silicon wafer before and after HDPA deposition provides additional evidence for the uniformity of the HDPA film. As expected, the surface of the sputtered and oxidized Ti−Nb layer on the polished silicon wafer (prior to HDPA deposition) is very smooth, although very fine (∼ 4 nm high) sputtering defects are occasionally observed (Figure 12a). The adsorbed HDPA layer (Figure 12b) closely mimics the topography of the substrate, and there is little apparent influence of the SAM overlayer on the overall roughness. This is in contrast to the AFM analysis of an octadecylphosphonic acid coating on the oxide surface of a simple titanium substrate reported by Schwartz and co-workers[16] which shows a distinct topography difference before and after phosphonic acid coating, that is, in their case, the overlayer does not uniformly reproduce the substrate topography.

Table 3. Intensities of the Methyl and Methylene Stretching Bands of OTS and HDPA Films (for CH_3 Peak, HDPA* = HDPA; for CH_2 Peaks, HDPA* = HDPA × 17/15)

IR signal		OTS	HDPA	HDPA*	OTS/HDPA*	
2959 cm^{-1} (CH_3)	area	0.612	0.68	0.68	0.90	0.96
	height	0.049	0.048	0.048	1.02	
2919 cm^{-1} (CH_2)	area	15.003	13.511	15.31	0.98	0.99
	height	0.698	0.622	0.7049	0.99	
2850 cm^{-1} (CH_2)	area	5.20	4.972	5.6349	0.92	0.93
	height	0.393	0.372	0.4216	0.93	

The difference in these two results may reflect differential reactivity introduced by the niobium oxide component of our alloy surface and/or differences in the coating methodology. While the Schwartz group[16] used an aerosol dosing with the advantage of less residual unbound coating material to be removed after coating but requiring up to seven repeated coating cycles, our deposition from solution (with solvent evaporation) found that two coating cycles were sufficient to establish a uniform, coherent, stable film.

Finally, the FTIR-ATR spectrum of HDPA on the TiO_2/Nb_2O_5 on the silicon wafer IRE was compared to the spectra of the hydrocarbon chains of an ordered siloxane-anchored monolayer, octadecyltrichlorosilane (OTS) on SiO_2/Si.[28]

Figure 13 shows the C−H region (2800−3000 cm^{-1}) of an OTS siloxane-anchored SAM and of HDPA on TiO_2/Nb_2O_5. The position of the methylene peaks (in both cases 2919 and 2850 cm^{-1}) is consistent with a well-ordered, near-crystalline packing of the hydrocarbon chains.[17] The intensities of the C−H stretching vibrations (as measured by the peak areas and by the peak heights) are listed in Table 3.

OTS and HDPA each have a single methyl group. The ratios of methylene/methyl carbons in OTS and in HDPA are 17/1 and 15/1, respectively (due to the differences in chain length). OTS on SiO_2/Si is known to be a true monolayer.[28] Thus, if the HDPA on TiO_2/Nb_2O_5 is also forming a monolayer, the intensities of their respective methyl peaks should be identical and their methylene peaks should also be the same after the HDPA peak is multiplied by 17/15. The column labeled HDPA* is normalized by this factor.

The important conclusion from these data is that the intensities of the OTS and HDPA (normalized) signals are always within 10% of each other, and just as the OTS on

(28) Ohtake, T.; Mino, N.; Ogawa, K. *Langmuir* **1992**, *8*, 2081.

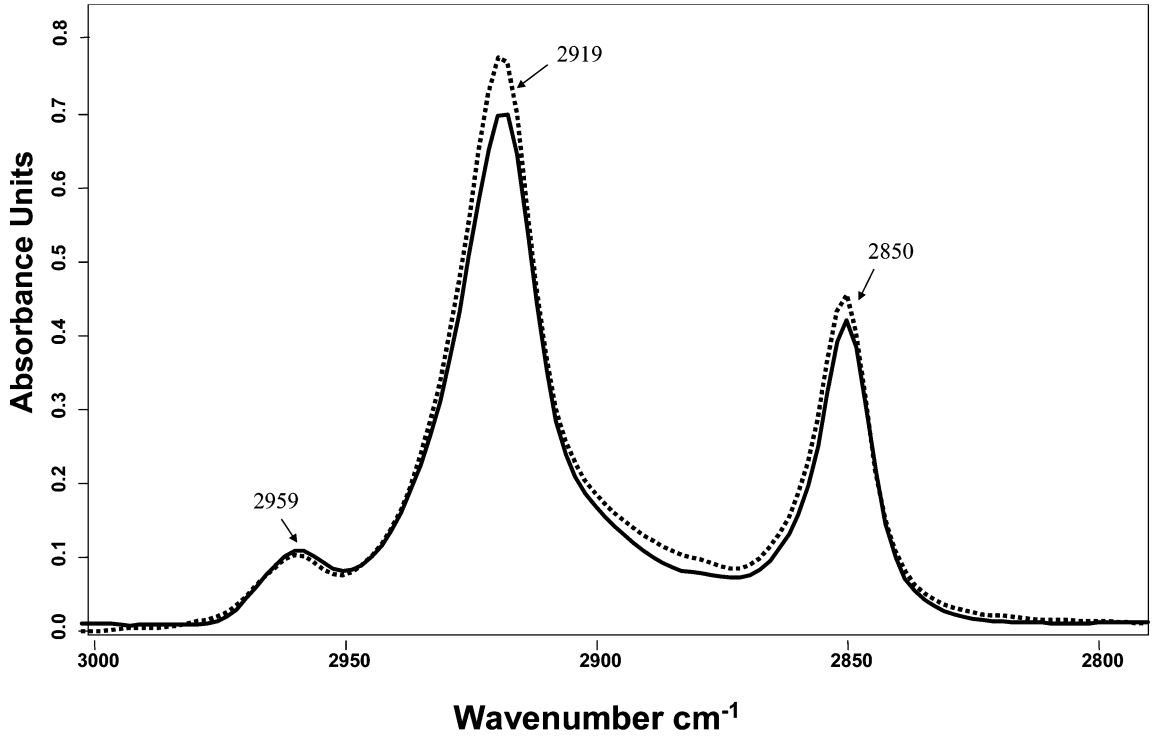

Figure 13. OTS monolayer on the silicon wafer (dotted line) and HDPA monolayer on the Ti−Nb deposited alloy (solid line).

SiO_2/Si is a monolayer, so too is HDPA on TiO_2/Nb_2O_5. These data provide independent confirmation for the monolayer-like thickness obtained by ellipsometry on this model oxide substrate and by XPS on the native alloy surface.

Conclusions

Electropolishing and anodic oxidation of Ti45Nb provides a surface which is a mixture of TiO_2 and Nb_2O_5. The anodization increases the thickness of the oxide layer and the surface roughness but does not change the grain boundaries of the substrate. The anodized surface is still highly reflective and is the preferred substrate for phosphonate SAM attachment. Wetting, ellipsometry, XPS, and FTIR measurements verify the presence of the phosphonate SAM. XPS analysis confirms the expected orientation of the alkyl phosphonate and the thickness of the monolayer film. Together with FTIR and AFM studies of an HDPA film on a thin film of TiO_2/Nb_2O_5 on a polished Si/SiO_2 surface, these data provide direct evidence for film thickness, uniformity, and order along with a detailed picture of the bonding at the interface between the SAM and the mixed oxide surface. The use of related SAMs (with functional groups at the other end of the alkyl chain) for surface modification of the Ti45Nb with biologically active materials is currently under investigation.

Acknowledgment. The authors want to thank Dr. Reuven Brener from the Solid State Institute, Technion for his assistance in XPS and AES analyses. We acknowledge the financial support of G.I.F. Research Grant N0 I-810-236.10/200 and of the Minerva Center for Tailored Biomaterial Interfaces at Bar Ilan University.

CM050477F